

---

# GALEX and Star Formation

Luciana Bianchi

**Abstract** Wide-field far-UV (FUV, 1344-1786Å) and near-UV (NUV, 1771-2831Å) imaging from *GALEX* provides a deep, comprehensive view of the young stellar populations in hundreds of nearby galaxies, shedding new light on the process of star formation (SF) in different environments, and on the interplay between dust and SF. *GALEX*'s FUV-NUV color is extremely sensitive to stellar populations of ages up to a few hundred Myrs, unambiguously probing their presence and enabling age-dating and stellar mass estimate, together with the characterization of interstellar dust extinction. The deep sensitivity, combined with the wide field-of-view, made possible in particular the discovery and characterization of star formation in extremely low-density, diffuse gas environments such as outer galaxy disks, tidal tails, low-surface-brightness galaxies (LSB) and dwarf Irregular galaxies, and of rejuvenation episodes in early-type galaxies. Such results provide several missing links for interpreting galaxy classes in an evolutionary context, extend our knowledge of the star-formation process to previously unexplored conditions, constrain models of galaxy disk formation, and clarify the mutual role of dust and star formation. We review a variety of star-forming environments studied by *GALEX*, and provide some model analysis tools useful for interpretation of *GALEX* measurements, and potentially as basic science planning tools for next-generation UV instruments.

**Keywords** Astronomical surveys — stars: star formation — galaxies: evolution — galaxies: stellar populations — ultraviolet: galaxies — interstellar dust: extinction

## 1 Introduction

The *Galaxy Evolution Explorer* (*GALEX*) has imaged in far-UV and near-UV a wide portion of the sky. Catalogs of hundreds of millions of UV sources enable advances in a variety of fields, from hot stellar objects in the Milky Way to QSOs (Bianchi et al. 2009) and star-forming galaxies, and provide a roadmap for future UV missions (see <http://dolomiti.pha.jhu.edu/uvsky>).

A deep, comprehensive view of the young stellar populations in hundreds of nearby galaxies, afforded by *GALEX*'s wide-field UV imaging, allows us to characterize their spatially-resolved and time-resolved recent star formation. In addition, star formation was revealed in extreme low-density environments, where it is elusive at other wavelengths. UV measurements of millions of more distant galaxies probe their evolution and the Universe's star-formation history (SFH) since redshift  $\sim 2$ .

In this review, we first recall the basic characteristics of *GALEX* data (Section 2.1) and of the UV-emitting young stellar populations which trace SF sites (Section 2.2), and we discuss dust extinction correction (Section 2.3). We review a number of environments where SF was discovered from UV imaging and was previously elusive, or thought to not possibly happen (low gas density conditions) in Section 3. We mention a few starburst places (Section 4) without attempting to be complete, which would be impossible. We do not address the abundant statistical studies of distant galaxy samples, aiming at reconstructing the star-formation history of the universe, because these are described elsewhere in this book. We provide, instead, a few sample diagnostic plots that may be of general use for a first interpretation of *GALEX* data, in particular for SF studies in nearby galaxies (Section 2.4), as well as for planning new UV and multi-wavelength observations.

---

Luciana Bianchi

Johns Hopkins University, Dept. of Physics & Astronomy, Baltimore, MD, USA

## 2 UV imaging of young stellar populations

### 2.1 GALEX data

*GALEX* performs wide-field ( $1.2^\circ$  diameter) imaging in two Ultraviolet (UV) bands simultaneously: FUV ( $\lambda_{eff}=1539\text{\AA}$ ,  $\Delta\lambda = 1344 - 1786\text{\AA}$ ) and NUV ( $\lambda_{eff} = 2316\text{\AA}$ ,  $\Delta\lambda = 1771 - 2831\text{\AA}$ ), with a spatial resolution of  $4.2/5.3''$  (FUV/NUV) (Morrissey et al. 2007), sampled with  $1.5'' \times 1.5''$  pixels. Its sensitivity reaches  $\sim 27.5\text{mag}/\square''$  with  $\approx 1,500\text{sec}$  exposures. *GALEX* has also a spectroscopic observing mode, which will not be addressed here.

The photometric system used in the *GALEX* archive is based on the AB magnitude scale<sup>1</sup> (see Morrissey et al. 2007). For most science analyses it is useful to combine *GALEX* data with corollary data at other wavelengths, especially the optical range where the Vega magnitude system is often used, therefore we give in Table 1 the transformation between the two systems in commonly used passbands, as computed by us from the filters' transmission curves, and the Vega spectrum.

**Table 1** Vega - AB magnitude transformation

Filter	$\text{mag}_{Vega} - \text{mag}_{AB} [\text{mag}]$
<i>GALEX</i> FUV	-2.223
<i>GALEX</i> NUV	-1.699
SDSS <i>u</i>	-0.944
SDSS <i>g</i>	0.116
SDSS <i>r</i>	-0.131
SDSS <i>i</i>	-0.354
SDSS <i>z</i>	-0.524
Landolt U	-0.694
Landolt B2/B3	0.125/ 0.123
Landolt V	0.004
Landolt R	0.180
Landolt I	-0.423
2MASS J	-0.901
2MASS H	-1.384
2MASS Ks	-1.852

*GALEX* performs nested surveys with differing sky coverage and depth, see Bianchi (2009) for a summary, Bianchi et al (2010, 2011a), Conti et al. (2011), and (Hutchings & Bianchi 2010a) for a description of the source content of currently released catalogs and sample science applications.

In total, with any level of exposure, over 46,000 galaxies within 100Mpc (velocity  $\leq 7000 \text{ km s}^{-1}$ ) are

now included in the *GALEX* imaging surveys, i.e. over 80% of the total number listed in Hyperleda database within such velocity limit and no culling criteria (Thilker, priv. comm.).

### 2.2 The UV-emitting young populations

Why is UV data sensitive to star formation? Young massive stars, hot, luminous, and short-lived, are the unambiguous tracers of star formation. They are luminous enough that they can be seen in distant galaxies. They evolve on fast timescales ( $\lesssim 10$  Myrs for O-type stars), therefore they also trace the original spatial structure of the star-formation episode, before the large complexes and stellar associations dissolve. They are very hot, therefore the UV wavelength range is ideal to detect and study them, because (i) UV colors are more sensitive to the temperatures of the hottest stars, enabling e.g. to discern O-types from late-O/early-B, while optical colors are saturated in this regime (e.g. Bianchi 2007), and (ii) UV colors provide precise age-dating of integrated stellar populations for ages less than 1Gyr. UV images give therefore an instant snapshot of young star-forming sites, uncomplicated by previous star-formation history, unlike longer wavelengths where multiple stellar generations contribute significantly to the light (Figs 1 and 2). Finally, UV fluxes are more sensitive to dust, which plays a major role in star formation, as will be discussed in Section 2.3.

Massive stars drive the chemical evolution of the Universe, enriching the interstellar medium (ISM) with nucleosynthesis products via supenova explosions and intense mass loss during AGB and planetary nebula phases, and driving the dynamical evolution of the ISM through highly supersonic stellar winds and mass loss up to  $\sim 10^{-5} M_\odot \text{ yr}^{-1}$  in their main sequence lifetime. Therefore, understanding their formation and characterizing them in a wide variety of environmental physical conditions (galaxy type, metallicity, gas content, dynamics including interaction events) helps our understanding of the overall evolution of the universe.

### 2.3 Characterizing dust extinction

#### 2.3.1 The mutual influence of dust and star formation

Dust is a minor component of the ISM, yet it has a major role in the formation of stars. In turn, hard UV radiation from massive stars can modify the dust grains' size distribution or coating. Extinction properties in the far-UV give information about the distribution of small dust grains in particular. It is important to understand the role of dust in the star-formation and ISM

<sup>1</sup> $m_{UV}(AB) = -2.5 \times \log(CTR_{UV}) + ZP$ , and zero-points  $ZP_{FUV} = 18.82$  and  $ZP_{NUV} = 20.08$ ; the countrate CTR is the dead-time-corrected, flat-fielded count rate in counts  $\text{s}^{-1}$

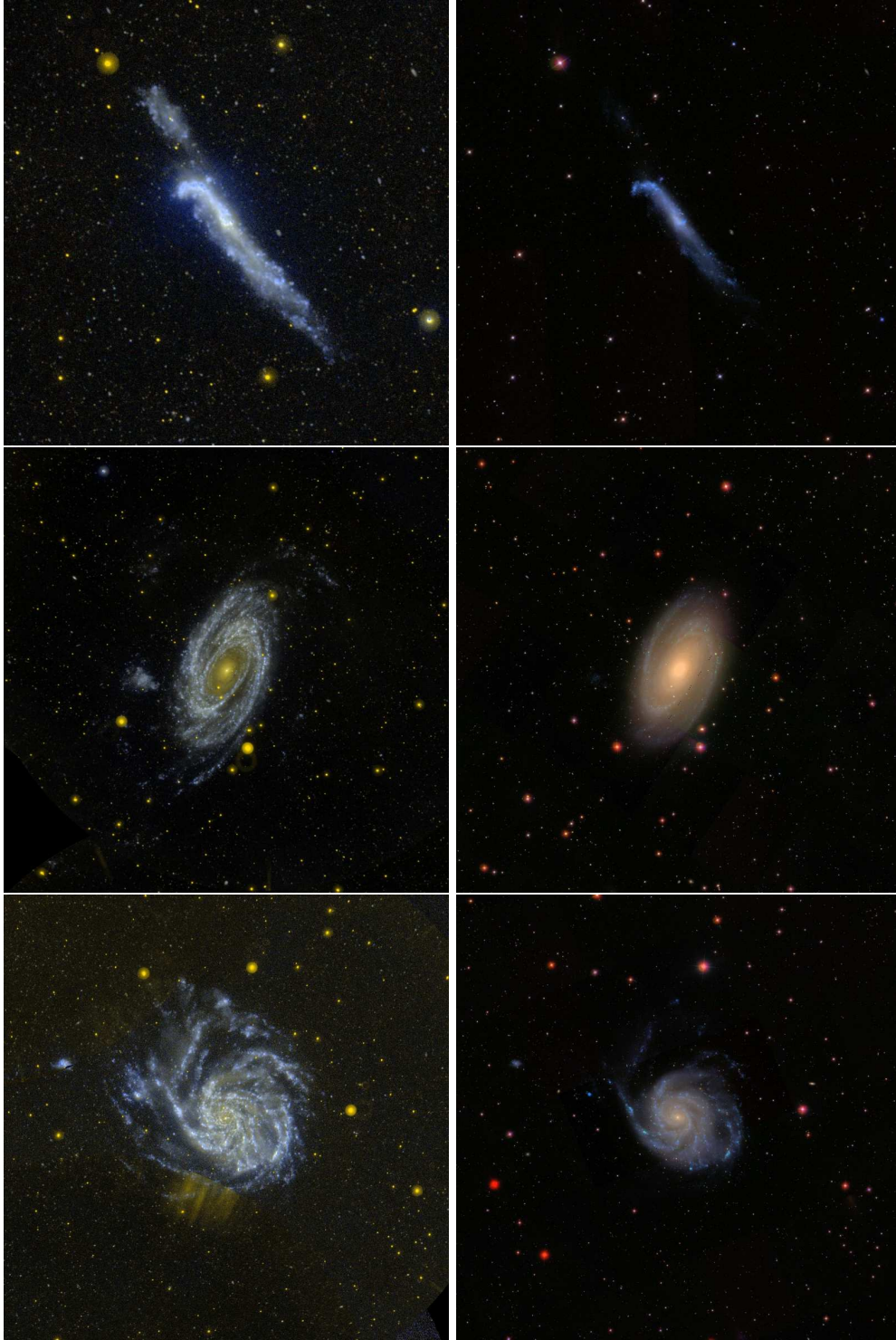


**Fig. 1** *GALEX* (left, FUV: blue and NUV: yellow) and optical (right, on the same scale) color-composite images of selected objects exemplifying the power of UV imaging for revealing young stellar populations. In particular, examples of dwarfs and tidal dwarfs inconspicuous in the optical are also shown, near bright galaxies. From the top: NGC 4656, M81, and M101.

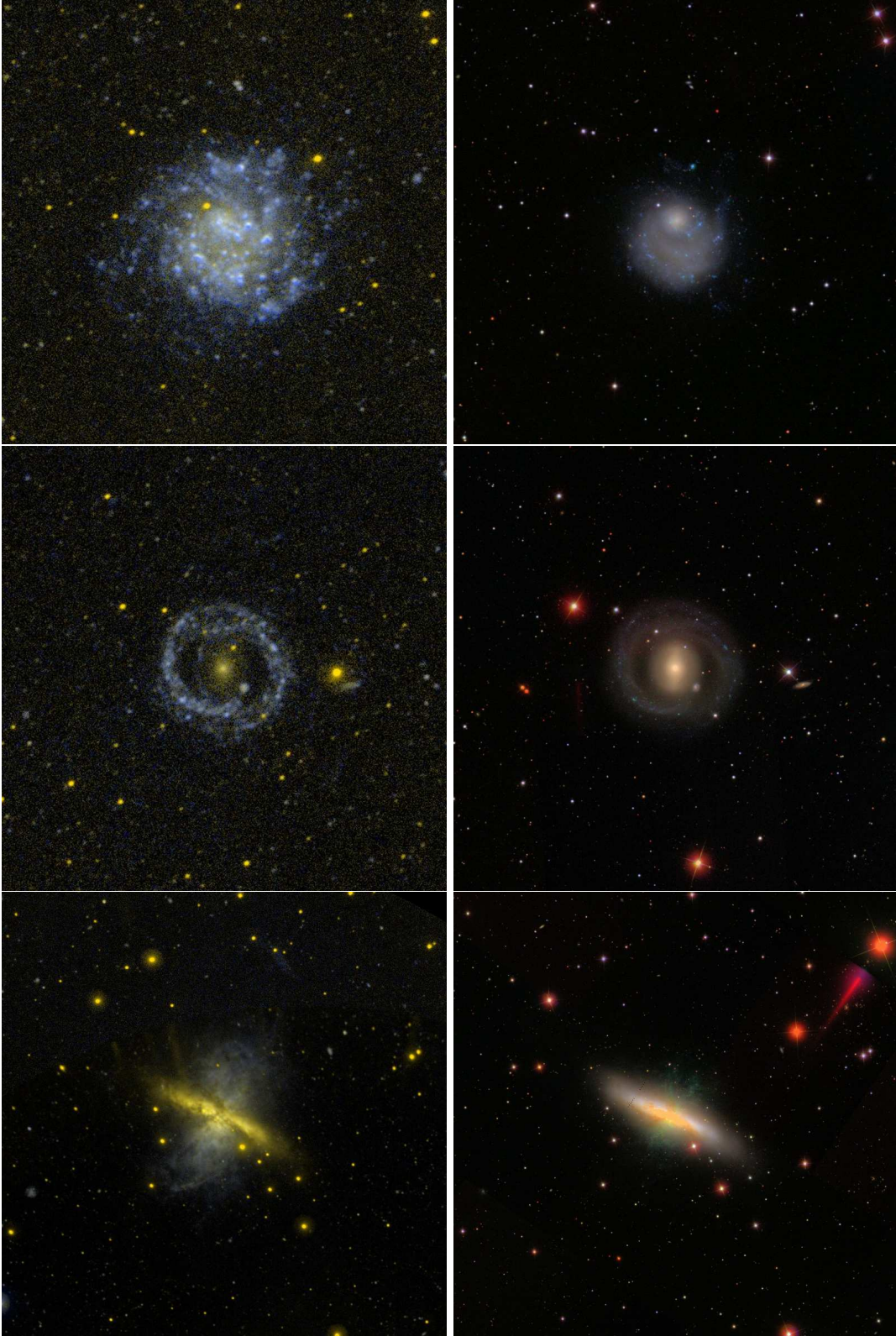


**Fig. 2** *GALEX* (left) and optical (right) color-composite images giving typical examples of: extended UV-disks (top, NGC5474), UV-emitting rings around early-type galaxies (middle, the SB0/a galaxy NGC5701) and halo UV emission (bottom: M 82, see Hoopes et al. 2005)

enrichment history of galaxies, and the relation of extinction to local and global galaxy properties such as metallicity and starburst intensity. It is also necessary to characterize dust extinction in various conditions, in order to interpret integrated properties of distant galaxies such as those measured by the *GALEX* surveys, to properly unreddened observed fluxes and correctly measure their energy budget and physical properties.

Extinction is a combination of scattering and absorption. Geometry, density, grain composition and UV radiation from hot stars are relevant parameters. Spectroscopic studies in the UV range show that in our Galaxy, an average extinction law can reproduce observed extinction curves (range  $1250\text{\AA} - 3.5\mu$ ) in a variety of dust environments (e.g. Mathis & Cardelli 1992, Cardelli et al. 1989), but sightlines through bright nebulae and dark clouds show significant deviations, which may result from the presence or absence of coatings on grains (e.g. Mathis 1994). In the LMC’s mini-starburst region LMC 2 the far-UV extinction is UV-steeper, and has a smaller  $2175\text{\AA}$  “bump”, than the Galaxy and other LMC locations (e.g. Misselt et al. 1999). The UV extinction is even steeper in the SMC. In M31 sightlines we found a MW-type curve but possibly a weaker  $2175\text{\AA}$  feature (Bianchi et al. 1996), and LMC-type extinction in M 33 (Bianchi et al. 2004, and in prep.). Although detailed studies are still scant, the ensemble of results suggests a strong but complex environmental dependence of dust properties. Generally, steeper UV extinction curves are found in starburst environments (e.g. Calzetti et al. 1995, 2005). However, quantitatively, extinction curve variations do not simply correlate with starburst activity in the same way in different galaxies.

Photometric studies of statistical samples of galaxies often use the ratio between IR and UV fluxes to estimate the UV-extinction. This process can be misleading because in detail, the SF sites emitting in UV hardly coincide with the IR-bright sites, since the latter trace the embedded (in dust) star formation ( $\sim$ few Myrs) while SF sites become UV bright after the dust has been largely blown away (Fig. 3). Similarly, comparison of  $H\alpha$  and UV fluxes can be misleading (except for youngest and most compact SF sites) because UV emission traces young populations for a  $\sim 10\times$  longer timescale than  $H\alpha$ , and moreover, when SF happens in a sparse region, ionizing photons may escape (while the UV emission, coming directly from the stars, will be unaffected by the spatial structure). Finally, methods that use the ratio of UV to IR fluxes for estimating UV dust attenuation (e.g. Cortese et al. 2008), assume that (i) the intrinsic slope of the UV spectrum or SED is known or constant, but the UV colors strongly vary

with age and metallicity (Fig. 5), and (ii) that far-IR fluxes and UV fluxes trace the same populations, which is mostly not the case (Fig. 3, also e.g. Efremova et al. 2011, Bianchi 2007). As a more detailed discussion is not possible here, we only mentioned the main caveats of such methods.

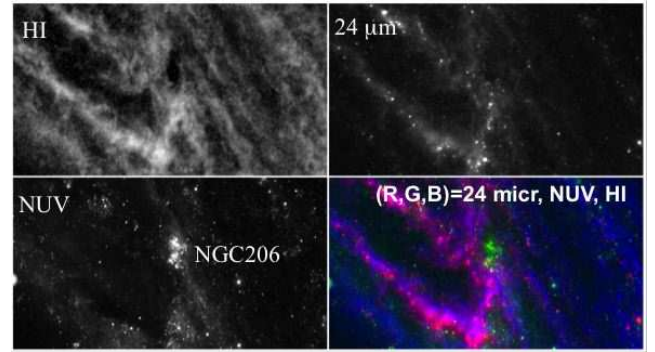


**Fig. 3** The bright SF region NGC206 in M31, shown in HI (upper left),  $24\mu$  (upper right), *GALEX* NUV (lower left), and composite ( $24\mu$ , NUV, HI: red/green/blue); UV emission is prominent where the hot stars have dissipated the dust, and conversely, IR emission from heated dust is prominent in embedded SF sites where the UV flux is completely absorbed

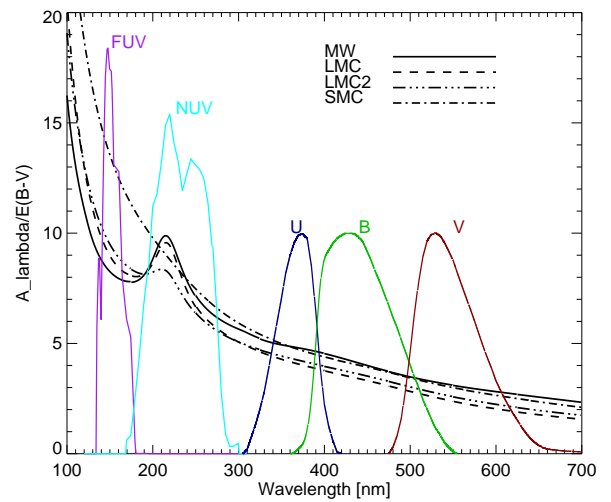


**Fig. 4** Selective extinction  $A_\lambda/E_{B-V}$  for some known, and largely differing, types of IS dust, shown with passbands of *GALEX* NUV & FUV, and classical U B V filters (the transmission curves are normalized arbitrarily for visibility).

### 2.3.2 Accounting for extinction by IS dust

An interesting property of the *GALEX* FUV-NUV color is that it is almost reddening-free for “typical

**Table 2** Broad-band reddening for different IS dust

	Type of selective extinction <sup>a</sup>			
	MW	LMC	LMC 2	SMC
$E_{FUV-NUV}/E_{B-V}$	0.11	1.08	2.00	4.60
$A_{FUV}/E_{B-V}$	8.06	8.57	9.02	12.68
$A_{NUV}/E_{B-V}$	7.95	7.49	7.02	8.08
$A_U/E_{B-V}$	4.72	3.96	4.11	4.61
$A_B/E_{B-V}$	4.02	3.26	3.46	3.85
$A_V/E_{B-V}$	3.08	2.34	2.54	2.93
$E_{U-B}/E_{B-V}$	0.70	0.70	0.66	0.76

<sup>a</sup> “MW” indicates the typical extinction curve for MW (from Cardelli et al. 1989), for LMC 2 the curve of Misselt et al. (1999) was used, for LMC average dust (outside LMC 2) and SMC, the extinction curves were taken from Gordon & Clayton (1998). The quantities for each broad-band are derived by applying the filter passbands to progressively reddened models for stars with  $T_{\text{eff}}$  between 30,000K and 15,000K, and comparing unreddened and reddened model colors with  $E_{B-V} = 0.4$ . The mean values are given, the dispersion is always less than 1% within this  $T_{\text{eff}}$  range)

MW”-type dust (and moderate extinction amounts). In fact, although the selective extinction  $A_\lambda/E_{B-V}$  increases towards shorter wavelengths, the *GALEX*  $\sim 1000\text{\AA}$ -wide NUV band entirely includes the strong broad absorption feature at  $2175\text{\AA}$  (Fig. 4), and therefore the overall absorption is not too different in the FUV and NUV bands (Table 2); in both it is much higher than in optical bands of course. In such case (MW dust) for example, ages of stellar populations could be derived from FUV-NUV model colors almost independently of extinction correction, averting a large source of uncertainty (which affects e.g. UV-optical colors). However, for UV-steeper extinction curves, such as LMC- and SMC-like curves, which are typical of young starburst regions, the FUV increase of the absorption  $A_\lambda$  is larger, and the  $2175\text{\AA}$  extinction “bump” less pronounced, making the observed FUV–NUV color highly sensitive to the amount, and type, of reddening.

Another consequence of using very-broad band photometry is that a reddening correction applied to the broad-band magnitude by using the value of  $A_\lambda$  at the  $\lambda_{\text{eff}}$  of the passband may not be accurate. Specifically, it becomes inaccurate when the slope of the source’s intrinsic spectrum is steep across the passband’s wavelength range. Therefore, for SED analyses with model colors, for example, we progressively redden the model spectra with increasing amounts of dust, then construct synthetic magnitudes for each reddened model, rather than dereddening the observed magnitudes with  $A_{\lambda_{\text{eff}}}$ .

From such model-magnitude grids, we compiled in Table 2 values of  $A_{FUV}/E_{B-V}$ ,  $A_{NUV}/E_{B-V}$  (and optical bands) and color excesses, by averaging the difference between synthetic magnitudes of reddened and unreddened models. These values are of general

utility, for moderate extinction amounts and a broad range of physical parameters. However, for e.g. cool stars, QSOs with redshift such that  $\text{Ly}\alpha$  crosses a passband, and other objects whose spectrum slope is steeply changing within the passband, the broad-band  $A_{\text{band}}/E_{B-V}$  value would slightly differ.

#### 2.4 Characterizing star formation: model diagnostics

In Figure 5 we show integrated-population synthetic models for coeval (SSP, or instantaneous burst) stellar populations, at representative ages. The effects of the most influential parameters are shown: metallicity and interstellar extinction. Other parameters include the IMF, upper mass limit, and the many ingredients in the recipe of stellar evolution; their effects would not be discernible on this scale. The plots illustrate very simply why FUV and NUV data offer great sensitivity to age-dating of the stellar populations, and are useful for interpreting observed colors of stellar clusters and other coeval populations. Model colors for galaxies (Elliptical and Spiral SHFs) are shown in Figure 6.

### 3 Star Formation in unsuspected or elusive sites

A combination of favourable factors conspires to facilitate discovery of star formation with *GALEX* in sites where it was elusive, or not expected. On one hand, the very low sky background and low foreground star counts in FUV increase the contrast of the UV-bright young populations, compared with imaging at longer wavelengths. Second, SF occurs when some pockets of gas happen to condense, even within diffuse low-density

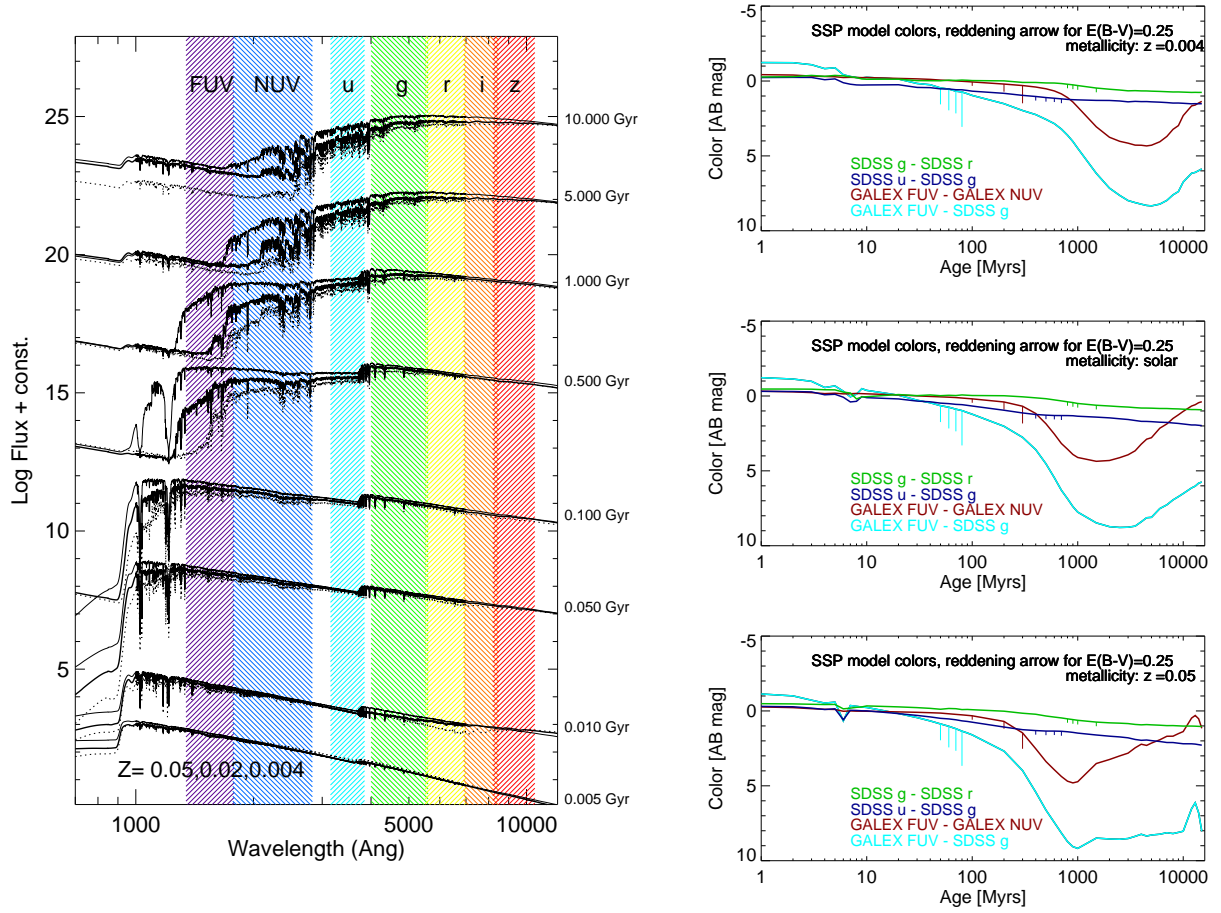


**Fig. 5** **Left:** SSP model spectra (Padua models, courtesy A.Bressan) at sample ages, for three metallicity values (solar: thick lines, supersolar: thin lines, subsolar: dotted lines). The plots explain the greater sensitivity of broad-band UV colors to ages of young stellar populations, compared with optical colors, and the relevance of metallicity in modulating the age dependence. Vertical bands indicate wavelength coverage of *GALEX* and SDSS filters. **Right:** broad-band SSP model colors including *GALEX* and SDSS bands, plotted as a function of age, for three metallicity values (given in the legend). The color excess for  $E_{B-V} = 0.25$  mag is shown on each color with vertical bars for four different types of extinction: MW-, LMC-, LMC2-, SMC-dust (bars from left to right). See section 2.3.

environments. Therefore, young stellar complexes are usually seen as compact clumps (often arranged along tidal tails, spiral density waves or compression fronts), then aging populations diffuse and disperse with time, fading below detectability even in very deep imaging in sparse outermost areas. Finally, O-type stars may account for over 90% of the total FUV emission of a very young population (SSP), and, for example, some UV-prominent outer rings which trace rejuvenation-induced SF in early type galaxies, emit  $\sim 75\%$  of the total galaxy FUV light, while containing only a few percent of the galaxy mass. This is why FUV imaging is sensitive to detect extremely low levels of SFR.

We review here some relevant environments where *GALEX* imaging uniquely enabled either the discovery, or a thorough characterization of SF, in most cases un-

expected according to prior wisdom (and data). For necessity of conciseness, rather than expounding on these findings, for which we refer to the original papers, we highlight the new paths opened by such discoveries, and the new questions they pose, that may be answered by follow-up programs.

- *Extended UV-disks (XUVD)*. Following the initial discovery of UV-emitting spiral-arm structures extending out to several times the optical dimension of M83 (Thilker et al. 2005) and NGC 4625 (Gil de Paz et al. 2005), Thilker et al. (2007) examined a sample of about 200 disk galaxies, and found XUVDs in  $\sim 30\%$  of them. XUVDs were classified in two basic types: Type 1 (found in Spirals of all types) and Type 2 (found in comparatively isolated galaxies, mostly late-type Spirals). A new larger sample now avail-

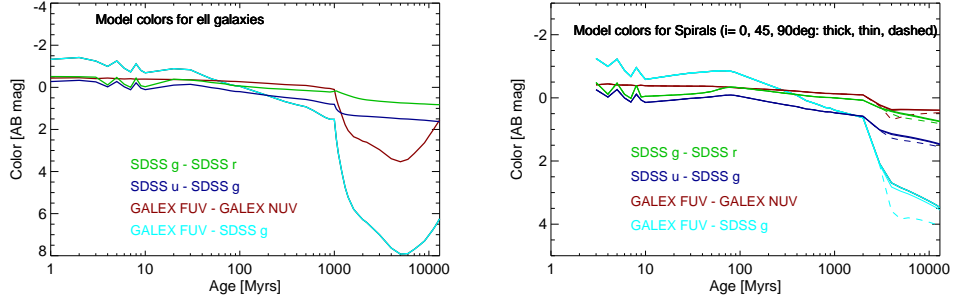


**Fig. 6** Synthetic galaxy population colors derived from models computed by us (Marino et al 2009) with the GRASIL code (Silva et al. 1998), which includes the age-dependent effects of internal extinction. Two typical SFHs are shown: for Ellipticals (left, passive evolution) and Spirals (right, for three different inclinations to show the extinction effects due to the disk geometry). Note the different magnitude scale

able ( $\sim 3500$  galaxies, under analysis) should help answer questions such as the role of the environment on the XUV phenomenon. Deep optical data, to be provided e.g. by *Pan-STARRS* (Panoramic Survey Telescope & Rapid Response System) in the next few years for a large enough sample, complementing the UV imaging, will clarify the relation of XUV to the galaxy optical surface-brightness profile, and enable study of radial color gradients for gaining insight in the SFR and SFH (Thilker et al. in prep).

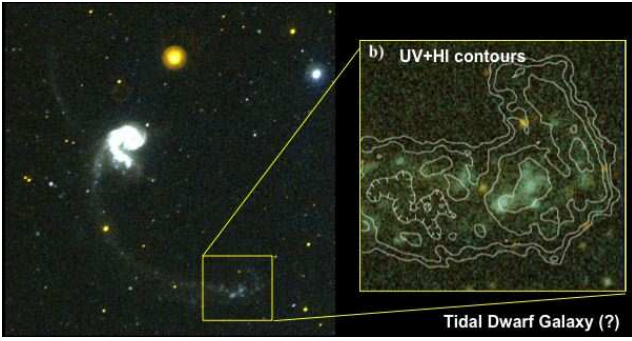


**Fig. 7** *GALEX* image of the “Antennae” interacting pair, with HI contours overlaid on an enlarged section. Figure adapted from Hibbard et al (2005)

- *Dwarfs, tidal Dwarfs and tidal tails.* In a hierarchical formation scenario, dwarf galaxies are relevant as building blocks; they are good searching grounds for pristine metal-poor material that allows us to explore conditions similar to earlier epochs in the universe; their number (or rather insufficient number) is one of the puzzles in dark matter (DM) investigations. In Local Group dwarfs, *GALEX* reveals conspicuous star formation even in cases believed to be rather isolate and not known to have suffered recent encounters (Bianchi et al. 2011b), and in faint dwarfs (e.g. Roychowdhury et al. 2010). An increasing number of

tidal dwarfs is also being discovered. Figure 7 shows the prototypical interacting galaxy pair, the Antennae, where UV imaging enabled age-dating of the populations along the tidal tails (indicating that star formation propagates in time towards outer regions) for comparison with the dynamics of the interaction (e.g. Hibbard et al. 2005, Zhang et al. 2010, Koribalski & López-Sánchez 2009) and indicates possible formation of tidal dwarfs caught in the act. In addition to tidal dwarfs, diffuse SF along tidal tails ( $\sim 100$  kpc scale) is prominent in UV and follows the gas distribution (e.g. Neff et al. 2005, Xu et al. 2005).

- *Star formation in primordial gas?* Probably the most extreme case where young UV-emitting stellar complexes have been found is the Leo ring, a  $\sim 200$  kpc wide gas structure presumed to be left-over from the formation of two central (well studied) galaxies ( $m-M=30$  mag). Detected in radio HI light, no deep imaging had previously succeeded to reveal signs of star formation within this gas reservoir. *GALEX* UV measurement of sparse clumps translate into a  $\Sigma_{SFR}$  of  $2 \times 10^{-4} M_{\odot}/\text{yr}/\text{kpc}^2$ , after some assumptions are made (Thilker et al. 2009). The relevance of this discovery remains to be fully assessed, mainly by constraining the metallicity of the gas and the stellar complexes, an arduous task with current instrumentation, given their faint luminosity in UV and undetectability at other wavelengths. Are the Leo ring UV-clumps (apparently lacking dark matter) a new way to form tidal dwarf galaxies? and in particular, with no pre-enrichment?
- *Rejuvenated ETGs*

Recent star formation in a number of nearby early-type galaxies (ETGs) has been revealed by UV-bright outer structures in wide-field UV imaging, by morphological distortions and spectral anomalies. Up to

30% of the ETGs imaged in the UV show rejuvenation signatures (e.g. Yi et al. 2005, Donas et al. 2007, Schawinski et al. 2007, Jeong et al. 2009, Rampazzo et al. 2007, 2011, Marino et al. 2010, 2011a,b). The nearest such example is the Lenticular galaxy NGC 404, where Thilker et al. (2010) discovered recent star formation in the outskirts, probably fueled by an external accretion episode (Fig. 8). Such outer rings often account for most of the FUV emission of the whole galaxy, although their mass is only a few percent of the total galaxy mass (Marino et al. 2011a,b). Mass estimates are currently based on *GALEX* FUV and NUV measurements only, because existing ground-based surveys only provide upper limits to these outer structures, which are inconspicuous at optical wavelengths. Therefore, the SFH cannot be constrained leading to large age and mass uncertainties. Deep optical imaging (planned), together with the FUV, NUV data, enabling the analysis of the whole SED of both the UV-bright ring structures (the ‘rejuvenation’ signatures), and the older, diffuse main galaxy stellar population should constrain SFH,

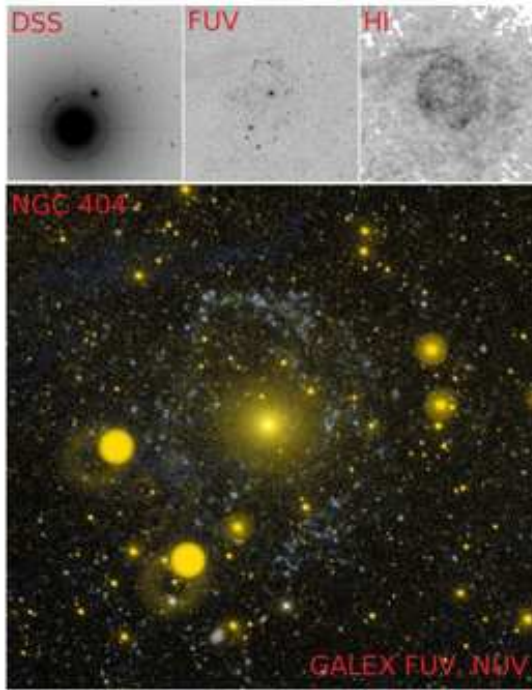


**Fig. 8** NGC404, the nearest example of early-type galaxy showing an outer ring of UV-emitting clumps, disclosing a young stellar population probably formed as a consequence of a tidally-induced “rejuvenation” (adapted from Thilker et al. 2010)

epochs and mass. The relative comparison between time–mass history of the major galaxy population (passively evolving) and the younger disk-like structures, together with dynamical analysis, information on gas content and distribution, and on environment, will clarify this important phase of galaxy evolution. This is yet another example where *GALEX* UV imaging calls for deeper optical data than the currently available surveys.

Questions still to be answered concern the origin(s) of such structures (secular, accretion, or both?); what provides the fuel and what dynamical factors trigger its collapse and star formation? In NGC404, HI data disclose an accretion episode that may have fueled the outer ring SF, but in other objects the cause is not known. What is the efficiency (of forming stellar mass) and what the incidence of such rejuvenation episodes, and their relevance in the galaxy evolution? We must wait for the answers in order to situate such objects in an evolutionary context, and clarify their relation to quiescent Ellipticals. The FUV excess in the SED of ‘rejuvenated’ ETGs place them in the so called ‘green-valley’ in the galaxy- UV-optical CMD (Thilker et al 2010, Marino et al. 2011b).

- *Low Surface-Brightness galaxies (LSB)*. What is the typical star-formation efficiency in LSBs? What is their star-formation history? Several hundred nearby known LSB observed (or planned) with *GALEX* may now provide answers (Thilker et al, in prep), since UV imaging proved to be more successful in detecting star formation than e.g.  $H\alpha$  surveys (e.g. Wyder et al. 2009, Boissier et al. 2008). Fig. 9 shows an example.



**Fig. 9** An example of LSB galaxy, UGC3642, seen with *GALEX* (left) and DSS2 (right). From Thilker et al. (in prep)

#### 4 The brightest sites of star formation

We focused mostly on the discovery of SF in previously elusive environments (extremely low gas density and SFR), to highlight UV-specific contributions to this

field. UV imaging is of course sensitive to measure ages and stellar masses of major starbursts. Here we only mention a few examples on the higher end of the SF scale.

- *Rings of fire and collisions* An efficient way to perturb/compress gas and induce SF on large (galactic) scales is galaxy-galaxy collision. The nearest example is the known “10 kpc ring” in M31 (the “ring of fire”), that simulations by various authors indicate to be a plausible product of an encounter between 10 and 210 Myrs ago (the estimated epoch varying among dynamical simulations). The ring is very prominent in UV imaging (Fig. 10), and it hosts an enhanced density of SF-complexes compared with the overall galactocentric gradient, concentrated around an age range that is consistent with the postulated collision (Kang et al 2009).



**Fig. 10** *GALEX* image of M31 (blue: FUV, yellow: NUV) showing the enhanced ring of star formation between  $\sim 9$  and 17 kpc (using  $m-M=24.47$ mag for M31)

- *UV-luminous galaxies* Extremely UV-luminous galaxies are being found with diverse sample selections, and seem to include objects with different properties, see e.g. Hoopes et al. (2007), Hutchings & Bianchi (2010b), and references therein.
- *UV emission from galaxy halos* Deep imaging of nearby galaxies often reveals diffuse UV-emitting halos, especially distinguishable in edge-on galaxies (Hoopes et al. 2005, see Fig. 2). The diffuse halo emission is consistent with being UV-light from the SF-disk scattered by dust in the halo, implying that intense starbursts may eject also dust (metals) along with gas into the intergalactic medium. Probing halos at fainter UV-flux levels would tell how efficiently even modest starbursts or ordinary SF can enrich the IGM.

## 5 Conclusions. UV vs other SF indicators

We have shown, with data and model predictions, that UV imaging is very sensitive to detect star formation down to extremely low levels; UV colors probe ages of stellar populations up to several hundred Myrs. By

comparison,  $H\alpha$  emission (i) traces the ionizing photons emitted by O-type stars, (or early-B, depending on the depth of the exposure) therefore fades at much younger ages, (ii) in sparse OB associations, photons may escape, in some cases only a thin  $H\alpha$  shell surrounding the young SF region may be seen, making it harder to trace the presence of ionizing stars in such cases. Dust emission e.g. at  $24\mu$  from embedded star formation reveals incipient SF bursts, and fades when dust is dissipated by the UV radiation and powerful winds from the massive stars, therefore it traces the earliest phases (few Myrs) of a SF episode, and complements the UV-detected young populations (Fig. 3). UV fluxes are much more affected by IS reddening than light at optical and IR wavelengths, and dust properties (and consequently, the UV extinction curve) vary in relation to environment, in particular to the presence of hot massive stars whose UV radiation may modify the dust grains. Therefore, extinction correction is a critical step in interpreting UV data (and may therefore be a source of uncertainty), and on the other hand, UV data provide information on dust that cannot be inferred from data at other wavelengths, and that is necessary to understand the star-formation process.

Finally, we point out that most of the discoveries exemplified in the “unsuspected” sites (as well as many other *GALEX* unexpected discoveries in different fields) were possible thanks to *GALEX*’s very large field of view. While HST provides detailed information (at superb resolution, and with a  $25\times$  larger collecting area) in selected tiny fields, *GALEX* has been a “discovery” instrument, path breaking for follow-up with HST, ground-based and future missions (e.g. WSO, Shustov et al. 2009, 2011). It has also shown that many more discoveries await in our future, from UV imaging.

**Acknowledgements** *GALEX* is a NASA Small Explorer, launched in April 2003. We gratefully acknowledge NASA’s support for construction, operation, and science analysis of the *GALEX* mission, developed in cooperation with the Centre National d’Etudes Spatiales of France and the Korean Ministry of Science and Technology. I am extremely grateful to David Thilker for useful discussions and for kindly providing some of the figures, and to the referee for a careful reading of the manuscript.

## References

- Bianchi, L., et al. 2010, Mon. Not. R. Astron. Soc., DOI: 10.1111/j.1365-2966.2010.17890.x
- Bianchi, L., Herald, J. et al. 2011a, this book
- Bianchi, L., Kang, Y.B., et al. 2011b, this book

- 
- Bianchi, L. 2009, *Astrophys. Space Sci.*, 320, 11
- Bianchi, L. et al. 2009, *Astron. J.*, 137, 3761
- Bianchi, L. 2007, in “UV Astronomy: Stars from Birth to Death”, eds. A. Gomez de Castro & M. Barstow, ISBN 978-84-7491-852-6, p. 65
- Bianchi, L., Bohlin, R.C., & Massey, P. 2004, *Astrophys. J.*, 601, 228
- Bianchi, L., et al. 1996, *ApJ*, 471, 203
- Boissier, S., et al. 2008, *Astrophys. J.*, 681, 244
- Calzetti, D. et al. 2005, *Astrophys. J.*, 633, 871
- Calzetti, D., et al. 1995, *ApJ*, 443, 136
- Cardelli, J.A. et al. 1989, *Astrophys. J.*, 345, 245
- Conti, A., Bianchi, L., Shiao, B., et al. 2011, *ApSS*, this issue
- Cortese, L., Boselli, A., Franzetti, P., et al. 2008, *Mon. Not. R. Astron. Soc.*, 386, 1157
- Donas, J. et al., 2007, *Astrophys. J. Suppl. Ser.*, 173, 597
- Efremova, B., Bianchi, L., Thilker, D., et al. 2011, *Astrophys. J.*, in press
- Gil de Paz, A. et al. 2005, *Astrophys. J. Lett.*, 619, L29
- Gordon, K. & Clayton, G. 1998, *Astrophys. J.*, 500, 816
- Hoopes, C. et al 2007, *Astrophys. J. Suppl. Ser.*, 173, 441
- Hoopes, C. et al 2005, *Astrophys. J. Lett.*, 619, L99
- Hibbard, J. et al. 2005, *Astrophys. J. Lett.*, 619, L87
- Hutchings, J. & Bianchi, L. 2011, *Astron. J.*, 140, 1987
- Hutchings, J. & Bianchi, L. 2010, *Astron. J.*, 139, 630
- Jeong, H. et al., 2009, *MNRAS*, 398, 2028
- Kang, YB, Bianchi, L, & Rey, S.-C. 2009, *Astrophys. J.*, 703, 614
- Koribalski, B & López-Sánchez, A 2009, *Mon. Not. R. Astron. Soc.*, 400, 1749
- Mathis, J.S. 1994, *Astrophys. J.*, 422, 176
- Mathis, J.S., & Cardelli, J.A. 1992, *Astrophys. J.*, 398, 610
- Marino, A. et al. 2011a, this book
- Marino, A. et al. 2011b, *Astrophys. J.*, submitted
- Marino, A. et al. 2010, *Mon. Not. R. Astron. Soc.*, DOI 10.1111/j.1365-2966.2010.17684.x
- Martin, D. C., et al. 2005, *Astrophys. J. Lett.*, 619, L1
- Misselt, K.A. et al. 1999, *Astrophys. J.*, 515, 128
- Morrissey, P. et al. 2007, *Astrophys. J. Suppl. Ser.*, 173, 682
- Neff, S. et al 2005, *Astrophys. J. Lett.*, 619, L91
- Rampazzo, R. et al. 2011, this book
- Rampazzo, R. et al. 2007, *Mon. Not. R. Astron. Soc.*, 381, 245
- Roychowdhury, S. et al. 2009, *Mon. Not. R. Astron. Soc.*, 397, 1435
- Schawinski, K. et al. 2007, *Astrophys. J. Suppl. Ser.*, 173, 512
- Shustov, B., Sachkov, M., Gomez de Castro, A. I., et al. 2009, *Astrophys. Space Sci.*, 320, 187
- Shustov, B., Sachkov, M., Gomez de Castro, A. I., et al. 2011, *Astrophys. Space Sci.*, this book
- Silva, L. et al. 1998, *Astrophys. J.*, 509, 103
- Thilker, D. et al. 2010, *Astrophys. J.*, 714, L171
- Thilker, D. et al. 2009, *Nature*, 457, 990
- Thilker, D., Bianchi, L., Boissier, S., et al. 2005, *Astrophys. J.*, 619, L79
- Wyder, T. et al, 2009, *Astrophys. J.*, 696, 1834
- Xu, C.K., et al. 2005, *Astrophys. J. Lett.*, 619, L95
- Yi, S.-Y. et al. 2005, *Astrophys. J. Lett.*, 619, L111
- Zhang, H. et al. 2010, *Mon. Not. R. Astron. Soc.*, 401, 1839